Comparison of Power Converters for Small-Scale Wind Turbine Operation

M. Pathmanathan, C. Tang, W.L. Soong and N. Ertugrul
University of Adelaide
Adelaide, Australia
mpathman@eleceng.adelaide.edu.au

***Abstract*- Small-scale wind turbines commonly use AC/DC converters such as rectifiers, switched mode rectifiers (SMRs) and inverters. Another power converter, the semi-bridge SMR has been researched for automotive applications, and is utilised by a number of small-scale wind turbine manufacturers. This paper applies a novel modulation technique developed for automotive applications of the semi-bridge SMR for Lundell and interior permanent magnet alternators to small-scale wind turbines utilising surface permanent magnet generators. The performance obtained using the semi-bridge SMR is compared to that obtained using single-switch SMRs and inverters.**

I. INTRODUCTION

A. Small-Scale Wind Turbines

In recent years, the level of interest in small-scale wind turbine generators has been increasing due to growing concerns over the impact of fossil-fuel based electricity generation. Small-scale wind turbines (<10kW) are particularly advantageous for power generation at a household level.

A small-scale wind turbine consists of a generator, a power electronic converter, and a control system, as shown in Figure 1. The generators used are usually permanent magnet machines, due to their high efficiency and self exciting properties. The power electronic converter topology used depends on the required output power and cost of the system. Control systems are used to control the rotational speed of small-scale wind turbines enabling them to operate with maximum efficiency. The next section discusses the commonly used power electronic converter topologies.

B. Power Electronic Converter Topologies

The cost of small-scale wind turbine systems is linked to the cost of the power electronics components, and their control

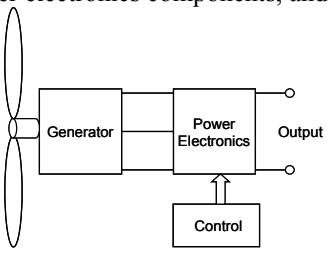

Figure 1: Small-scale wind turbine generator model

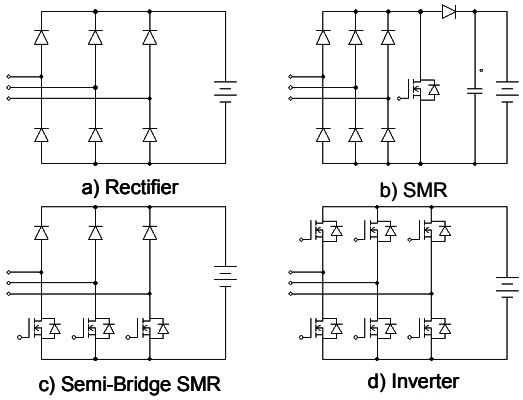

Figure 2: Circuit diagrams of a rectifier (a), single-switch SMR (b), semi-bridge SMR (c) and inverter (d)

complexity. Figure 2 shows four common power electronic topologies: the rectifier, single-switch switched mode rectifier (SMR), semi-bridge SMR and inverter. The inverter can also be called a full-bridge controlled rectifier, but this paper refrains from doing so in order to maintain consistency with the nomenclature used in earlier papers [1-5].

Inverters can extract the greatest output power from a generator at a given speed. Unfortunately, the inverter's cost is also highest due to the number of switches, more complex control strategies and the need for rotor position information [1]. The rotor position information can be obtained by optical encoders, resolvers or Hall-effect sensors. These sensors increase the topology cost and reduce its reliability. Although sensorless algorithms can be used to eliminate physical rotor position sensors, these algorithms require complex calculations and usually need a digital signal processor and additional feedback signals to implement.

The rectifier needs no position or speed information, and only utilises diodes as opposed to the transistors in an inverter. This greatly reduces the component cost of this power electronic converter. Unfortunately, the output power obtainable at low speeds with a rectifier is significantly lower than with an inverter. Additionally, this topology does not allow any control over output power or generator torque and speed, meaning that maximum power point tracking is not possible.

This trade-off between cost and performance in power electronic converter choice has led to alternative topologies, such as the single-switch SMR to be investigated [4]. This converter has both lower cost of components and control

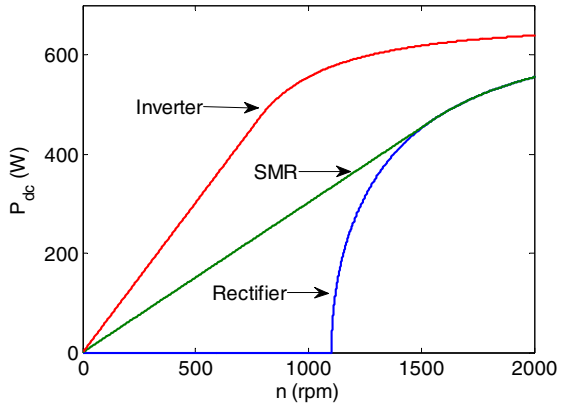

Figure 3: Simulated output power for a permanent magnet generator with inverter, single-switch SMR and rectifier loads with a high inductance permanent magnet generator model operating into a 12 V load.

complexity than the inverter, and provides greater power at low generator speeds than the rectifier. Figure 3 shows a comparison of simulated ideal output power obtained using a rectifier, single-switch SMR, and inverter for an example small-scale wind turbine generator.

In reference [1] extensive tests were conducted on the use of a single-switch SMR as a power converter for small-scale wind turbines. This study showed that the duty cycle of the transistor in the SMR could be controlled to provide enhanced output power compared to the rectifier at low generator speeds, and also to control generator torque and hence wind turbine speed at high wind speeds.

Whilst the single-switch SMR provides a significant low speed power improvement over a rectifier, it still produces less power in this range than an inverter. It is possible to achieve greater output power than the single-switch SMR with a semi-bridge SMR at a lower cost than an inverter by using the phase advance modulation technique, which is detailed below.

C. Phase Advance Modulation Method

The aim of this modulation strategy is to produce a phase shift which reduces the angle between the back-emf and phase current waveforms [3]. This effectively produces a leading power factor like an inverter and results in greater output power being produced.

References [2] and [3] used this modulation technique and demonstrated significant performance increases for automotive applications. While some commercial wind turbine power electronics units use the semi-bridge SMR topology, it is not known whether they utilise the conventional method of modulation for single-switch SMR converters [1], or the technique specified by [3]. To date, no research has been published on the viability of the phase advance technique when used with a wind turbine.

The method utilised by [3] involves modulating each transistor in the semi-bridge SMR individually (see Fig. 2c). Figure 4 shows phase current and effective voltage waveforms resulting from this modulation method for one phase of the semi-bridge SMR. Note that the waveforms

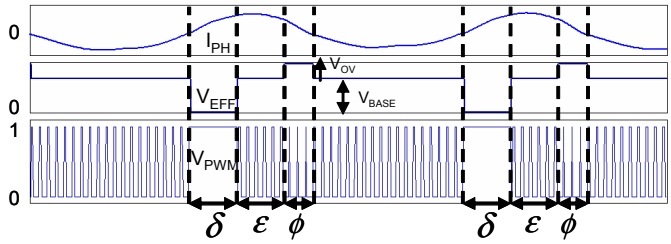

Figure 4: Modulation scheme intervals showing phase current I_{PH}, SMR effective voltage V_{EFF} and transistor gate drive signal V_{PWM} [3]

corresponding to the other two phases would be identical, but shifted by 120°.

As is illustrated in the figure, there are three separate modulation intervals while the phase current is positive. During interval δ the duty cycle of the transistor in the semi-bridge SMR is unity, which in turn causes the effective phase to ground voltage (V_{EFF}) to be set to zero, causing the phase current waveform (I_{ph}) to increase rapidly. During interval ε the duty cycle is set at the optimal value for conventional SMR modulation, causing V_{EFF} to rise to V_{BASE}. Finally during interval ϕ the duty cycle is driven lower than the value during ε, effectively causing V_{EFF} to rise to a value V_{OV} which is higher than V_{BASE}. This in turn causes the phase current waveform to fall more rapidly.

This paper investigates the use of a semi-bridge SMR modulated by the phase advance technique in wind turbine applications by performing simulations based on the parameters of a commercial 400 W wind turbine generator.

II. Analytical Comparison of Single-Switch SMR and Inverter Performance

The single-phase equivalent circuit of a surface PM generator consists of an AC back-emf voltage source in series with a winding inductance and winding resistance. Power electronic converters are required to transform the AC electrical power produced by the generator into DC power which can either be stored in batteries for later use or transferred to the power grid using a DC/AC converter. In addition, such converters must be controlled in order to extract the maximum possible output power under varying wind speed conditions.

For a system to achieve maximum output power, its input and output impedance must be matched. In the system considered, the output impedance of the generator consists of series resistance and inductance. The type of load impedance used in this model varies according to the power converter used. In the case of an inverter, the effective load impedance consists of a variable resistance and capacitance, while for a single-switch SMR the load consists of a variable resistance (see Fig. 5). The SMR is represented as a resistance because its input rectifier forces the AC input voltage and current waveforms to be in phase.

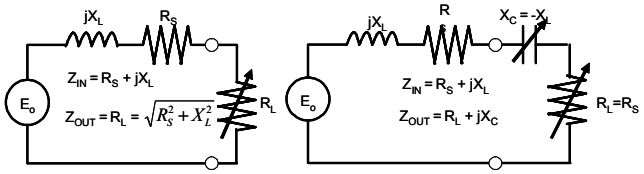

Figure 5: Optimal SMR and Inverter loads of PMG

The inverter has more control flexibility and can control the input current to have any desired phase angle with respect to the input voltage. Given the generator output impedance is inductive, maximum output power is generally obtained with the current leading the voltage. This behaviour is analogous to that of a passive load consisting of a series resistance and capacitance.

In order to obtain maximum power from the SMR, its effective value of load resistance must be equal to the magnitude of generator impedance which can be given by:

$$R_L = \sqrt{R_S{}^2 + X_L{}^2} \tag{4}$$

Here X_L is the reactance of the inductor, and is given by:

$$X_L = \omega L \tag{5}$$

In the inverter case however, the resistive part of output impedance is matched by a resistor of the same value, while the inductive part is cancelled by a series capacitor of equal reactance. The value of the capacitor is given by:

$$C = \frac{1}{\omega X_L} \tag{6}$$

The power produced by a SMR is lower than that generated by an inverter because its output current *I* and voltage *V* are restricted to being in phase, as indicated in [1]. This is illustrated by Figure 6c, for a high inductance model of a PMG (6a), which ignores the effects of stator resistance. In contrast, under maximum output power conditions, the inverter (Figure 6 b) can force the current vector **I** to lead the voltage **V** at low speeds to keep the current in phase with the induced voltage **E**. This leading power factor causes the inverter to generate approximately twice the power of a SMR at low speeds.

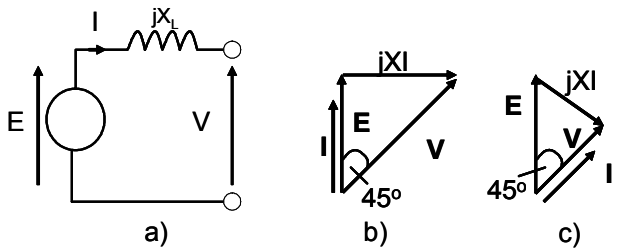

Figure 6: High inductance equivalent circuit for a PMG (a), inverter phasor diagram at low speeds (b) and SMR phasor diagram at low speeds (c) [1]

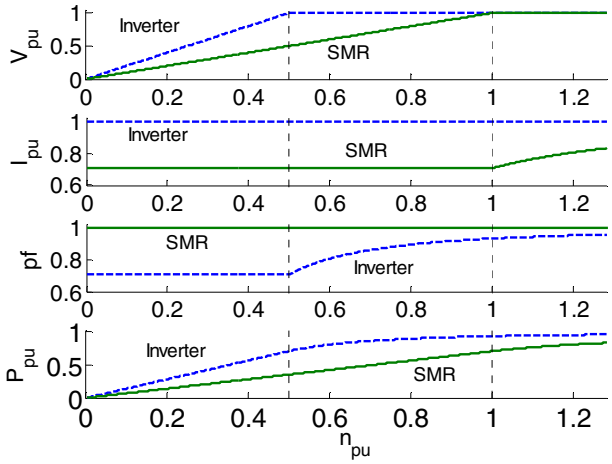

Figure 7: Generator voltage, current, output power factor and power for inverter and SMR cases under maximum output power conditions

Figure 7 shows the generator's output voltage, current, power-factor and power when operating with an inverter and SMR under maximum power conditions. It is clear from this figure that the SMR produces half the generator output voltage, approximately 0.7 times the current and 1.4 times the power factor of the inverter at low speeds. Given that P = VIcos(ϕ), where cos(ϕ) is the power factor, thus the SMR produces half the output power of the inverter at low speeds.

III. Practical Single-switch SMR Modulation Results

The simulations presented in Figure 7 ignored the effects of generator stator resistance, in order to present an ideal model. This section will examine the effects of stator resistance on the voltage, current and power obtained with a single-switch SMR.

A commercial 400 W permanent magnet generator was used as the basis for a series of simulations and experiments on the performance of single-switch SMR modulation. The parameters of the generator are presented in Table 1.

TABLE 1
Permanent Magnet Generator Equivalent Circuit Parameters

Characteristic	Value
Rated Power	400 W
DC output Voltage	12 V
Number of Poles	12
Stator Resistance (R_s)	0.0986 Ω
Synchronous Inductance (L)	0.19 mH
Magnet Flux Linkage (ψ_M)	0.308 ($V_{phase\ RMS}$)/(c/s)

The voltage-current (VI) locus is a useful tool for describing the operation of a SMR. It shows the locus of the output voltage and current of the generator with a variable resistive load corresponding to operation with a single-switch SMR.

The effect of stator resistance on the generator AC current I_{ph} is shown in Figure 8, where the analytically computed AC VI loci are shown for the ideal case (R_S = 0) and the case where R_S equals the measured value of stator resistance (0.0986Ω). The voltage and current measured for this case are the AC waveforms produced by the generator. It is clear that

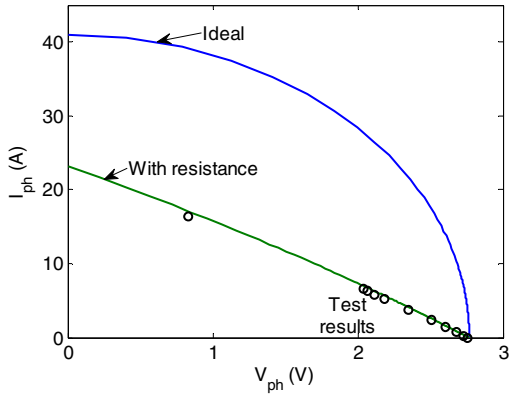

Figure 8: AC VI Loci for the generator in Table 1 for the ideal ($R_S = 0$) and the case where $R_S = 0.0986\ \Omega$ at a speed of 565 rpm. Experimental results for the latter case are shown as circles.

of the stator resistance reduces the short-circuit current significantly at this speed. Experimental results are also presented. These experiments and simulations were conducted at a generator speed of 565 rpm. This speed was chosen in lieu of the generator's rated maximum rotational speed of 1800 rpm because experimental testing revealed that the short-circuit current at speeds above 565 rpm was too high for extended operation.

Figure 9 shows the results obtained for the DC VI locus of the generator at a speed of 565 rpm. The voltage and current used in this VI locus were taken from the DC output of the SMR. Results from time-stepping simulations conducted in PSIM® are included in this graph for comparison. The analytical and PSIM models used take into account a voltage drop of 0.85 V per diode. It is clear that the time-stepping simulated results are closer to the experimental values than the analytical curve. This discrepancy is due to inaccuracies present in the analytical model's computation of the DC voltages and current.

A comparison of the DC output power corresponding to Figure 9 is shown in Figure 10. The inclusion of stator resistance causes a power reduction of approximately 30% when compared to the ideal case.

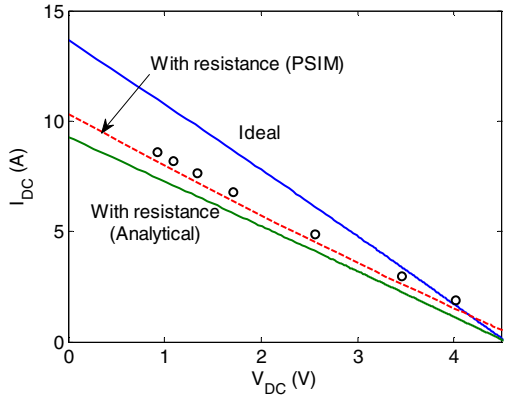

Figure 9: DC VI Loci for the generator in Table 1 for the ideal case, and for the case where $R_S = 0.0986\ \Omega$ for a speed of 565 rpm. Experimental (circles) and PSIM simulated results are also shown for the latter case.

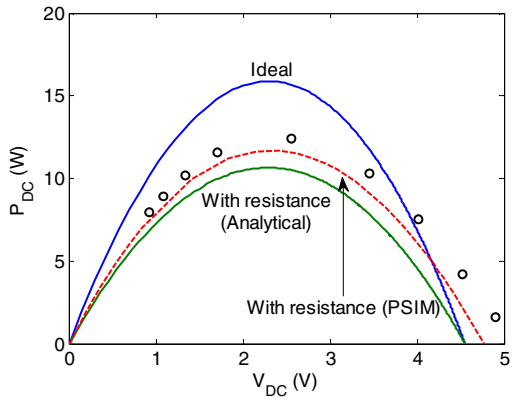

Figure 10: DC Power as a function of DC voltage for the generator in Table 1 for the ideal case, and where $R_S = 0.0986\ \Omega$ at 565 rpm. Experimental (circles) and PSIM simulated results at $R_S = 0.0986\Omega$ are also shown

Finally, Figure 11 shows the comparison of the ideal generator output power and the output power obtained using $R_S = 0.0986\Omega$ versus speed. The PSIM simulations and experimental results are included for comparison, and show a close correspondence to the analytical model with stator resistance included. These results clearly show that stator resistance has a significant effect on the output power for this generator.

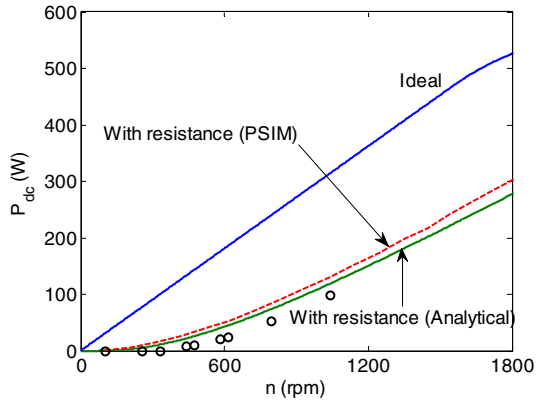

Figure 11: DC Power as a function of generator rotational speed for the ideal case, and where $R_S = 0.0986\Omega$. Experimental (circles) and PSIM simulated results at $= 0.0986\Omega$ are also shown

IV. Phase Advance Modulation of a Semi-Bridge SMR

A series of simulations based on the phase advance modulation technique were conducted in order to predict the performance increase obtainable for this generator.

A. Ideal Simulations

A PSIM model was used to perform simulations which determined the maximum power obtainable as the control angles δ and ϕ were varied (see section I C). Figure 12 shows the model used for the initial simulations. It should be noted that an ideal representation of a PMG without any stator resistance was used, and the diodes and transistors modelled in the semi-bridge SMR were initially ideal devices.

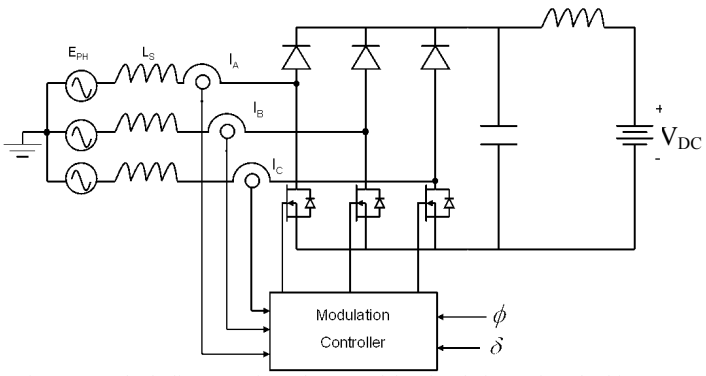

Figure 12: Block diagram of topology used for simulations of method in [3]

The ideal output power curves of a PMG using a conventionally modulated SMR and inverter as a function of the generator's phase current at 1000 rpm are shown in Figure 13. In addition, scatter plots are given in the figure, which represent the calculated output power and corresponding phase current values obtained by modulating a semi-bridge SMR with phase advance method for δ and ϕ values ranging between 0° and 180° in steps of 10°. Several points of interest are marked as A to D on this figure, which are explained in Table 2.

TABLE 2
POINTS EXAMINED IN PHASE ADVANCE SIMULATIONS

Point	Description
A	Conventional SMR modulation
B	Maximum power obtainable with phase advance modulation when phase current is limited to current at point A
C	Maximum power obtainable with phase advance, while keeping phase current at its rated value
D	Maximum power obtainable with phase advance without any current limitations

It is apparent that while the phase advance technique produces greater power than the SMR, the phase current at which it produces maximum power (point D) is greater than that at the corresponding point for conventional SMR modulation (point A). Operation under such conditions may not be desirable, since the large values of phase current may cause excessive heat dissipation.

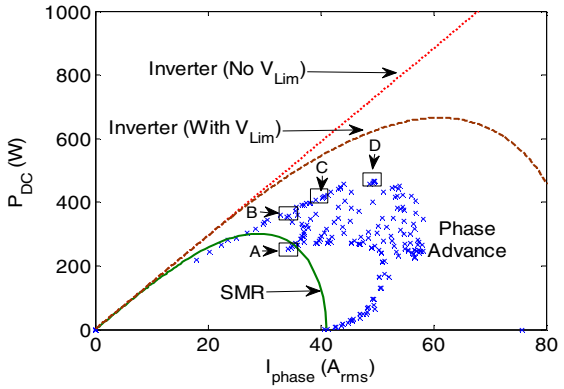

Figure 13: Output power vs phase current for simulations of conventional SMR modulation, phase advance modulation, and an inverter used with an ideal PMG model at 1000 rpm

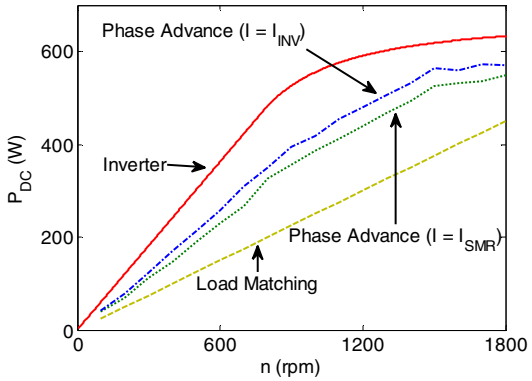

Figure 14: Output power vs generator speed for simulations of SMR, phase advance (limited to rated SMR and inverter currents) and inverter operation with an ideal PMG model

Due to these issues, it was decided to take the maximum power point for phase advance modulation as the largest power reading for phase current values equal to or below either the phase current obtained using conventional SMR modulation (point B), or the rated inverter current (point C) at that speed. Simulations were conducted at speeds ranging from 100-1800 rpm in order to find the maximum power point under these conditions for the phase advance technique. The results are shown in Figure 14.

It is clear from these simulations that the phase advance method of modulation provides a significant improvement over conventional SMR modulation when generator stator resistance and power converter losses are neglected. Simulations taking these quantities into account must be conducted in order to obtain a more accurate representation of this technique's performance under real life conditions. These are presented in the next section.

B. Non Ideal Simulations

For an accurate simulation of the system, stator resistance and power converter losses should be taken into account. The losses were assumed to consist of a 0.85 V voltage drop for diodes, and a 2.1 mΩ resistance for transistors. Figure 15 shows simulations of the output power obtained as phase

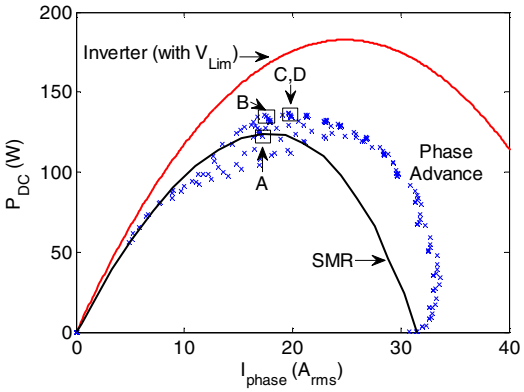

Figure 15: Output power vs phase current for simulations of conventional SMR modulation, phase advance modulation, and an inverter used with a non-ideal PMG model at 1000 rpm

current was varied at 1000 rpm for conventional SMR operation, phase advance modulation, and an inverter. The same points that were examined in Figure 13 are also shown for comparison. It is apparent that the maximum power obtainable with all three topologies is considerably less than that obtained using ideal simulations. Additionally, the phase current value at which the maximum power point occurs for the phase advance case is lower than the rated current, unlike in Figure 13.

Similarly, the new simulation model was run between 100-1800 rpm in order to find the maximum power obtainable whilst keeping phase current under the conventional SMR value at that particular speed using the phase advance method. The results given in Figure 16 indicate that the power gains obtained by the phase advance method are considerably less under the non-ideal conditions. The curve for phase advance output power with the phase current limited to the SMR phase current value for a given speed was not shown since it was very similar to the curve for phase advance power with phase current limited to the inverter's phase current value.

The unsatisfactory power improvements obtained for the phase advance simulations with stator resistance included are consistent with the power losses observed in Figure 11 for conventional SMR modulation. The results of these simulations show that high values of stator resistance significantly reduce the maximum output power obtainable from a permanent magnet generator under both conventional and phase advance SMR operation.

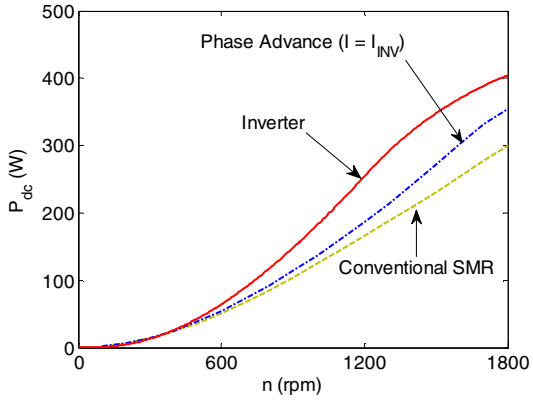

Figure 16: Output power vs speed for an inverter and simulations of conventional and phase advance SMR operation with current limited to either that obtained with a conventional SMR, or an inverter for a non-ideal PMG model

V. Conclusions

This paper has shown that the phase advance modulation technique is capable of producing greater power than conventional semi-bridge rectifier (SMR) modulation without increasing the value of phase current in a small-scale wind turbine's surface permanent magnet generator (PMG). Therefore, it can be concluded that the phase advance modulation technique in a semi-bridge SMR can potentially be a low-cost alternative to an inverter based systems utilising PMGs in small-scale wind turbines.

The next stage in the research is the experimental implementation of the hardware system. The phase advance modulation technique will be implemented by a circuit designed in [2] which uses a microcontroller to generate the pulse-width modulated waveforms required to drive the transistors in the semi-bridge SMR. Once the simulations provided in this paper have been verified, tests will be conducted on a generator with a lower values of stator resistance in order to determine the performance increases which can be obtained with such a machine.

Acknowledgments

This project is sponsored by an Australian Research Council (ARC) grant DP0878530. The assistance provided by workshop staff at the School of Electrical and Electronic Engineering is gratefully acknowledged. The author would also like to thank Chong-Zhi Liaw for the design of the experimental setup used.

References

[1] D.M. Whaley, W.L. Soong and N. Ertugrul "Investigation of Switched-Mode Rectifier for Control of Small-Scale Wind Turbines", IEEE Industry Applications Society Annual Meeting 2005, Vol. 4, pp 2849-2856.

[2] C.Z. Liaw, W.L. Soong and N. Ertugrul "Low-Speed Output Power Improvement of an Interior PM Automotive Alternator", IEEE Industry Applications Society Annual Meeting 2006, Vol. 1, pp 27-34.

[3] J. Rivas, D. Perreault, T. Keim, "Performance Improvement of Alternators with Switched-Mode Rectifiers", IEEE Transactions on Energy Conversion, Vol. 19, No. 3, September 2004 pp. 561-568.

[4] W.L. Soong, N. Ertugrul, "Inverterless high power interior permanent magnet automotive alternator", IEEE Transaction on Industry Applications, Vol. 40, No. 4, July/August 2004 pp. 1405-1412.

[5] C.Z. Liaw, D.M. Whaley, W.L. Soong, N. Ertugrul, "Investigation of Inverterless Control of Interior Permanent Magnet Alternators", IEEE Transactions on Industry Applications, Vol. 42, No. 2, March/April 2006 pp. 283-289.

[6] D.J. Perreault, V. Caliskan, "Automotive Power Generation and Control", IEEE Transactions on Power Electronics, Vol. 19, No. 3 May 2004 pp. 618-630.

[7] J. Darbyshire, C.V. Nayar, "Modeling, Simulation and Testing of Grid Connected Small Scale Wind Systems", Australasian Universities Power Engineering Conference 2007, pp 1-6.

[8] E. Hau, "Wind Turbines Fundamentals, Technologies, Application, Economics", Vol 2, Springer Berlin Heidelberg, 2006.